

# Theoretical Studies of AlGaAs-GaAs Multiple-Quantum-Well Single Channel Waveguide Defined by Ion-Implantation-Induced Intermixing

Michael H. F. Chu<sup>a</sup> and W. C. Shu<sup>b</sup>

<sup>a</sup>Department of Electrical and Electronic Engineering, University of Hong Kong,  
Pokfulam Road, Hong Kong

<sup>b</sup>Department of Mathematics, Hong Kong Baptist University, 224 Waterloo Road,  
Kowloon, Hong Kong

## Abstract

A simple and accurate model is presented for the analysis of ion-implanted AlGaAs-GaAs multiple-quantum-well (MQW) single channel waveguide. Our model proposed that the interdiffusion is vacancy enhanced. So we simulate the interdiffusion mechanism by solving the coupled diffusion equation of vacancy and interdiffusion numerically. The modal propagation constants full width half-maximum (FWHM) and field profiles of the guided modes of the waveguide are solved numerically using a semi-vectorial wave equation.

MQW optical waveguides defined by ion-implantation-induced intermixing are shown to have similar optical properties as conventional dielectric rib optical waveguide. They also provide a more flexible control over the waveguiding characteristics by changing parameters such as periods of MQW layers, mask width, ion implant energy, and diffusion time.

**Index Terms:** Ion implantation, semiconductor waveguides, quantum well devices and semiconductor superlattices

## 1. INTRODUCTION

The selective intermixing of III-V Compound semiconductor quantum-well (QW) structures have been widely employed to realize various photonic devices [1]. This technique offers a planar technology to alter the bandgap energy, refractive index and other optical properties of the QW materials. Impurity-induced intermixing by diffusion, ion implantation, and impurity-free vacancy diffusion can enhance the interdiffusion rate of diffused QW's by a large extent [2]-[4]. In present work, ion implantation is used as it provides an accurate depth control of the intermixing region.

Recently, multi-quantum well (MQW) waveguides have played a significant role in the fabrication of photonic integrated circuits [5]. The refractive index difference between the diffused and as-grown area in AlGaAs/GaAs interdiffused MQWs has been demonstrated to be large enough to permit simple waveguide [6]. Later, interdiffusion of an AlGaAs/GaAs MQW was used to produce low-loss waveguides especially at the wavelengths near to the absorption edge of the MQW [7]. The fabrication of a buried-stripe optical waveguide by ion implantation has been shown [8], which has been used to realize simple and efficient waveguide polarizers because of the optical birefringence exhibited [9]. Subsequently, a 90% polarization conversion in an AlGaAs/GaAs superlattice waveguide without employing phase matching techniques has been obtained [10]. High-energy implantation has also been applied to realize AlGaAs/GaAs single mode waveguides for 1.15  $\mu$ m light and room temperature lasers [11]. The first optical channel waveguiding in a MQW structure in which the channel waveguide is formed by compositional mixing induced by Focus Ion Beam (FIB) implantation has been demonstrated [12].

There has been a lot of effort spent in studying the electronic and optical properties of ID modified AlGaAs/GaAs MQW structures, but rather little has been reported so far about the detailed theoretical

waveguiding properties of this type of device. The purpose of this chapter is to investigate into this area. A detailed model of a two-dimensional 1D waveguide structure is considered here. The effects of the structure's dimensions, the implantation parameters and the propagating condition, on the waveguiding properties, and the optical confinement factor are examined. Special attention has been paid to the conditions for ensuring single-mode propagation.

As waveguiding structures of present studies are made of diffusion, the structures are having inhomogeneous refractive index profiles [13]. Analytical solution to the wave equation cannot be obtained. Therefore, numerical analysis becomes essential. A number of numerical methods have been developed to solve for the modal propagation constants and field profiles of the guided modes of optical waveguiding structures with arbitrary cross section and refractive index profile [14]. A model for the ion-implanted single channel waveguide consisting of AlGaAs-GaAs MQW is developed. By solving the semi-vectorial wave equation, the quasi-vector-guided modes of the single channel waveguide are analyzed. This method is accurate down to modal cutoff. While varying parameters such as waveguide separation, mask width, and ion implant energy, the waveguiding properties of waveguides at different diffusion times are examined. In Section II, a model for the MQW waveguides and its mathematical formulations are described. Numerical results are presented in Section III.

## 2. MODELING

Masked ion-implantation technique is used to alter the bandgap and, hence, the refractive index of the as-grown square QW material in selective regions. The mask-covered area has higher refractive indexes than the implanted area, thus producing lateral confinement of light and a two-dimensional waveguide is formed [15]. The schematic of the structure to be analyzed is shown in Fig. 1 It is composed of AlGaAs-GaAs MQW layers on a thick AlGaAs buffer layer grown on a GaAs substrate. Mask is placed on top of the whole structure which is exposed in air. Impurity  $\text{Ga}^+$  ions are injected at high energy, followed by Rapid Time Annealing at  $950\text{ }^\circ\text{C}$ . Single channel waveguides are formed as a consequence.

Assuming the mask has an infinitely steep edge and is thick enough to avoid penetration, the as-implanted impurity and vacancy concentration profile can be simulated by using SRIM96 program. The SRIM96 program simulates the behaviour of a number of specific atoms/ions of certain energy and dose in microscopic view.

The Interdiffusion Mechanism is vacancy-enhanced. So the mechanism can be simulated by solving the coupled set of the diffusion equations between vacancies and the lattice site Al. [16] Noted that the interaction of the interstitial atoms was included in the diffusion equation for the equation for the vacancies by adding onto it a recombination term of the form  $(V - V_{eq})/\tau$ , where  $V_{eq}$  is the thermal equilibrium vacancy concentration at the annealing temperature and  $\tau$  is a phenomenological time constant that describes the decay of the transient vacancy distribution. The equations can be written as

$$\frac{\partial V(x, y, t)}{\partial t} = D_V \nabla^2 V(x, y, t) - \frac{V(x, y, t) - V_{eq}(x, y, t)}{\tau} \quad (1)$$

$$\frac{\partial C(x, y, t)}{\partial t} = \nabla [D_{Al}(x, y, t) \nabla C(x, y, t)] \quad (2)$$

where  $D_V$  is the vacancy thermal equilibrium diffusion coefficient,  $V(x, y, t)$  is the vacancy concentration,  $C(x, y, t)$  is the concentration of lattice site Al and the  $D_{Al}$  transient diffusion coefficient is given by

$$D_{Al}(x, y, t) = D_{Al, eq} \frac{V(x, y, t)}{V_{eq}(x, y, t)} \quad (3)$$

where  $D_{Al,eq}$  is the thermal equilibrium Al diffusion coefficient.

The square of the diffusion length  $L_d(x,y)$  can be calculated by integrating  $V(x,y,t)/V_{eq}(x,y,t)$  with respect to time

$$L_d^2(x,y) = D_{Al,eq} \int_0^T \frac{V(x,y,t)}{V_{eq}(x,y,t)} dt \quad (4)$$

where T is the annealing time.

The diffusion length profile now has much more grid points in the y-direction than the number of QW's, the profile is sampled again into regions equivalent to a single QW, and the mean value in each region is chosen. In this way, each QW is matched with a specific diffusion length  $L_d$ . The Al concentration profile  $w(y)$  of a single QW with well width  $L_z$ , is given by

$$w(y) = w_o \left\{ 1 - \frac{1}{2} \left[ \operatorname{erf}\left(\frac{L_z + 2y}{4L_d}\right) + \operatorname{erf}\left(\frac{L_z - 2y}{4L_d}\right) \right] \right\} \quad (5)$$

where  $w_o$  is the initial Al concentration. A developed model is adopted to find the refractive index profile  $n_r(x,y)$  of the diffused QW structure [17].

In order to analyze the guiding properties of the waveguide, the wave equation has to be solved numerically. For a translationally invariant real refractive index profile  $n_r(x,y)$ . The electric field E can be described by the vector wave

$$\nabla^2 E(x,y) + k^2 n_r^2(x,y) E(x,y) + \nabla [E(x,y) \frac{\nabla n_r^2(x,y)}{n_r^2(x,y)}] = 0 \quad (6)$$

where  $k = 2\pi/\lambda$  is the free-space wavenumber and  $\lambda$  is the free-space wavelength. Consider the transverse electric field components  $E_x$  and  $E_y$  propagate in the z-direction with phase change  $\exp(j\beta z)$  where  $\beta$  is the associated propagation constant, (7) is reduced to two coupled equations for  $E_x$  and  $E_y$  as follows:

$$\frac{\partial^2 E_x}{\partial x^2} + \frac{\partial^2 E_x}{\partial y^2} + (k^2 n_r^2 - \beta^2) E_x + 2 \frac{\partial}{\partial x} (E_x \frac{\partial}{\partial x} \ln n_r + E_y \frac{\partial}{\partial y} \ln n_r) = 0 \quad (7)$$

$$\frac{\partial^2 E_y}{\partial x^2} + \frac{\partial^2 E_y}{\partial y^2} + (k^2 n_r^2 - \beta^2) E_y + 2 \frac{\partial}{\partial y} (E_y \frac{\partial}{\partial y} \ln n_r + E_x \frac{\partial}{\partial x} \ln n_r) = 0 \quad (8)$$

The first three terms in (7) and (8) represent the scalar wave equation, the fourth term is a polarization correction, while the last term corresponds to the coupling between  $E_x$  and  $E_y$ . For quasi-TE modes,  $E_y = 0$  and for quasi-TM modes,  $E_x = 0$ . Solutions of quasi-TE modes will be given in the present studies by solving the semi-vectorial wave equation for  $E_x$ .

$$\frac{\partial^2 E_x}{\partial x^2} + \frac{\partial^2 E_x}{\partial y^2} + (k^2 n_r^2 - \beta^2) E_x + 2 \frac{\partial}{\partial x} (E_x \frac{\partial}{\partial x} \ln n_r) = 0 \quad (9)$$

(9), which can be transformed into an eigenvalue problem, is solved by an eigen-solver to obtain the eigenvalues  $\beta$  and eigenvectors  $E_x$ .

For a given refractive index profile,  $n_r(x,y)$ , the normalized propagation constant b is calculated by

$$b^2 = \frac{n_{eff}^2 - n_{cl}^2}{n_{co}^2 - n_{cl}^2} \quad (10)$$

where  $n_{cl}$  and  $n_{co}$  are the refractive index of the cladding and core respectively.

### 3. Numerical Results and Discussion

Optical waveguides with different geometrical and optical parameters are investigated. All calculations are done for quasi-TE modes, considering that TM-mode should give similar results. The total lateral width of waveguide,  $2L$ , is  $4.0\mu\text{m}$ . The thickness of  $\text{Al}_{0.3}\text{Ga}_{0.7}\text{As}$  buffer layer and MQW layers are  $3.0$  and  $1.0\mu\text{m}$ , respectively. The MQW layers consist of 30 periodic layers of 100-A GaAs wells and 100-A  $\text{Al}_{0.3}\text{Ga}_{0.7}\text{As}$  barriers. The mask width ( $2a$ ) is varied from  $1\mu\text{m}$  to  $3\mu\text{m}$ . The buffer is introduced to avoid the diffusion of impurities from the substrate layer. The schematic is shown in Figure 1

Implantation is performed at room temperature with implant dose  $N_0 = 5 \times 10^{12} \text{ cm}^{-2}$  and 220keV implant energy as to minimize damage. A typical vacancy concentration profile in  $\text{Ga}^+$  ion implantation obtained from the TRIM simulation is shown in Figure 3(a).

For the computation of postimplantation Al concentration profile, the time step in (2) is taken as  $0.0001\text{s}$ . To solve for the quasi-TE wave equation (9), the modal electric field is expanded into a Fourier Series using 30 harmonics in both x- and y-directions, which give rise to an eigenvalue problem of  $900 \times 900$  matrix elements. A sample of the two-dimensional refractive index profile is shown in Fig. 3(b) with an annealing time of  $30\text{s}$ . The detail of the implementation of the proposed model is shown in the flow chart in Fig. 2.

Prior to diffusion, there is no guiding mode in the MQW Structure due to a uniform lateral refractive index profile. As interdiffusion proceeds, the refractive indices of the implanted region for TE mode operation fall gradually while the mask covered region remains the same except near the mask edges. From a certain diffusion time onwards, the difference of refractive index between this two regions,  $\Delta n_r$ , is sufficiently large that guided mode is observed to occur. The increase of  $\Delta n_r$ , is demonstrated in Fig. 3(b).

Guiding of the fundamental (even) mode first occurs, followed by the excited (odd) guided mode. The field profile is determined by FDM with total QW layers thickness of  $1\mu\text{m}$ . A symmetric field profile  $E_{11}$  is shown Figure 4. The contour levels (Figure 4(b)) are 10% intervals of the maximum field amplitude. The optical wave is mostly confined in the high refractive index MQW region, only a little evanescent wave being present in the buffer layer. A strong confinement due to the air, whose refractive index is 1, is clearly shown.

Each guided mode is accompanied by propagation constant. The normalised propagation constants of these even and odd modes as a function of annealing time is plotted in Figure 5, for the cases where the mask width is  $2\mu\text{m}$ , the implant energy is 220keV and the operating wavelength is  $0.85\mu\text{m}$ . The  $\Delta T_{SM}$  is defined as the time duration between  $t_1$  and  $t_2$ , which is the time for single mode operation. This happens as interdiffusion proceeds ( $t_1$  increases),  $\Delta n$  also increases and beyond a certain time  $t_2$  when the  $\Delta n$  gets large enough, a second mode will start to guide. An example of these values can be readily extracted from Figure 5, where the first guided mode  $t_1$  occurs after  $5.1\text{s}$  of the interdiffusion time and the time duration of single-mode operation  $\Delta T_{SM}$  is  $7\text{s}$ .

Two major waveguide parameters, the propagation constant  $\beta$  and the full width half maximum (FWHM), and the effect of interdiffusion on these parameters will be addressed. The interdiffusion extent is characterised by annealing or interdiffusion time. The variables include the mask width, the implantation energy, the periods of quantum wells and the operating wavelength.

Attention is now turned to the effect of mask width. In the case of a 30 periods of QWs and operating wavelength  $0.85\mu\text{m}$ , the plot of normalised propagation constant and FWHM against time are shown in Fig. 6(a) and Fig.(b). This shows that a shorter diffusion time is required as the mask width enlarges, but it also shows a decrease in the quality of confinement in term of FWHM.

As the number of quantum wells is increased from 20 to 50 with mask width  $2\mu\text{m}$  and operating wavelength  $0.85\mu\text{m}$ , the plot of normalised propagation constant and FWHM against time are also shown in Fig. 7. In general, as the thickness of the guided region increases, the guiding mode appears earlier. However, an improvement in FWHM is shown in fewer periods of QWs.

The effect of wavelength is next considered by examining operation at two wavelengths ( $0.85\mu\text{m}$  and  $0.9\mu\text{m}$ ). At implantation of  $220\text{keV}$  a mask width  $2\mu\text{m}$  and 30 periods of QWs, the plot of normalised propagation constant and FWHM against time are also shown in Fig.8. A better FWHM can be obtained with a shorter wavelength, which is shown in Figure 8. The reason for this may concern the properties of AlGaAs/GaAs MQWs—the refractive index difference ( $\Delta n$ ) of AlGaAs/GaAs MQWs at operating wavelength  $0.85\mu\text{m}$  and  $0.9\mu\text{m}$  are different. The maximum  $\Delta n$  was shown at about  $0.85\mu\text{m}$  [4]. It implies that the optimal FWHM with short interdiffusion time waveguide can be achieved if the operating wavelength is chosen to be  $0.85\mu\text{m}$ .

The influence of varying the implant energy with constant mask width  $2a = 2\mu\text{m}$ , 30 periods of QWs and operating wavelength  $0.85\mu\text{m}$  is now studied. The plot of normalized propagation constant and FWHM against time are shown in Fig. 9. As the implant energy is increased, an improved (larger)  $t_1$  can be obtained and a better confinement can be obtained with higher implantation energy.

$t_1$  and  $\Delta T_{SM}$  also show a decreasing trend if the number of quantum wells is increased which corresponds to the depth of the guiding region. A set of data is used to illustrate this. This is the case when the implantation energy is  $220\text{keV}$ , mask width is  $2\mu\text{m}$  and operating wavelength is  $0.9\mu\text{m}$ . The fundamental mode appears quickly while  $\Delta T_{SM}$  decreases. It can be concluded that the annealing time can be reduced by enlarging the guiding region. On the other hand, it is discovered that both the  $t_1$  and the  $\Delta T_{SM}$  increase with the increase of implantation energy. It implies that to shorten the annealing time, lower implant energy is preferred. But if a long duration of single-mode operation is wanted, the waveguide should be fabricated with high implant energy. However, attention should be paid to the damage of the waveguide, which have great effect on the scattering loss. The absorption coefficient of the analyzed waveguide was found to be  $49.41\text{cm}^{-1}$ . The total loss is given by  $\alpha_{total} = \alpha_s + \alpha_{core}\eta + \alpha_{clad}(1-\eta)$  where  $\alpha_s$  is the average scattering loss,  $\eta$  is the optical confinement factor. The optical is already determined to be about  $\eta \approx 70\%$ . The total loss found is to be  $50.1\text{cm}^{-1}$

#### 4. CONCLUSION

A model has been developed for studying MQW single channel waveguide defined by ion-implantation-induced intermixing. It enables a quasi-TE/TM analysis of the propagation characteristics of the waveguides. Knowledge of the modal propagation constants, field profiles and confinement of the guided modes have been gathered to facilitate the design of MQW single channel waveguide. The effects of ion implantation and geometric parameters on the waveguiding properties of the single channel waveguide are analysed. The most important finding is that better optical confinement can be obtained within the waveguide by using a smaller mask. A single transverse mode operation from a waveguide is essential for most applications, because it facilitates higher coupling efficiency with optical fibres and eliminates noise and instability due to mode competition. A better way to enhance the optical confinement is by increasing the implant energy or decreasing the number of quantum wells. However, both of these conditions require a longer interdiffusion time.

#### Acknowledgements

The authors would like to thank Dr. E. Herbert Li of the University of Hong Kong for his invaluable advice on this field of optoelectronics and J. F Ziegler of IBM Research for his technical support of providing the useful simulation program SRIM96.

#### REFERENCES

1. B. L. Weiss. Ed., "Special issue on quantum well mixing for optoelectronics," *Opt. Quantum Electron.*, vol.23, pp.S799-S994. 1991.

2. I. Harrison, "Impurity-induced disordering in III-V multi-quantum well and superlattices," *J. Mat. Sci.. Mat. In Electron.*, Vol. 4 pp 1-28, 1993
3. W Freiman, R. beserman, Yu. L. Khait, M. Shaanan, K. Dettmer, F R. Kessler, "Ion-implantation and thermal-anneal-induced intermixing in thin Si/ Ge superlattices," *Phys. Rev. B.*, vol. 48(4), pp. 2282-2291, 1993.
4. I. Gontijo, T Krauss, R. M. De La Rue, J. S. Roberts, and J. H. Marsh, "Very low loss extended cavity GaAs/AlGaAs lasers made by impurity-free vacancy diffusion," *Electron. Lett.*, vol.30, pp. 145-146, 1994.
5. S. Charbonneau, P.J. Poole, P G. Piva, G. C. Aers, E. S. Koteles, M. Fallahi, J.-J. He, J. P McCaffrey, M. Buchanan, M. Dion, R. D. Goldberg, I. V Mitchell, "Quantum well intermixing for optoelectronic integration using high energy ion implantation", *J. Appl. Phys.*, vol. 78, pp. 3697-3705, 1995.
6. F Julien, P D. Swanson, M. A. Emanuel, D. G. Deppe, T A. DeTemple, J J. Coleman and N. Holonyak, Jr., "Impurity-induced disorder-delineated optical waveguides in GaAs-AlGaAs superlattices", *Appl. Phys. Lett.*, vol. 50 (14), pp. 866-868, 1987
- 7 Y Suzuki, H. Iwamura and O. Mikami, "TE/TM mode selective channel waveguides in GaAs/AlAs superlattice fabricated by SiO<sub>2</sub> cap disordering.", *Appl. Phys. Lett.*, vol. 56(1), pp.19-20, 1990.
8. B. L. Weiss and J. Roberts, "Disorder-induced buried-stripe optical waveguides in GaAs/AlGaAs MQW material.", *Electronics Letters*, Vol. 25 (10), pp. 653-654, 1989.
9. E. Kapon, N. G. Stoffel, E. A. Dobisz, and R. Bhat, "Birefringent channel waveguides defined by impurity-induced superlattice disordering", *Appl. Phys. Lett.*, vol. 52 (5), pp. 351 -353, 1988.
10. T Wolf, C. L. Shich, R. Engelmann, K. Alavi and J Mantz, "TE-to-TM mode conversion in GaAs/AlGaAs Superlattice waveguide,", *Elect. Lett.*, vol. 25(18), pp.1221-1223,1989.
11. D. R. Myers, Kyu Lee, T Hausken, R. J Simes, H. Ribot, F Laruelle, and L. A. Coldren, "High-energy argon-ion implantation for waveguide formation in (AlGa)As/GaAs multilayers," *Appl. Phys. Lett.*, vol. 57 (20), pp. 1180-1185, 1990.
12. M. Kumar, V Gupta, G. N. DeBrabander, P Chen, J. T Boyd, A. J. Steckl, A. G. Choo, H. E. Jackson, R. D. Burnham, and S. C. Smith, "Optical Channel Waveguides in AlGaAs Multiple-Quantum-Well Structures Formed by Focused Ion-Beam-Induced Compositional Mixing.", *Photo. Tech. Lett.*, vol. 4 (4), pp. 435-438, 1993.
13. R. K. Lagu and R. V Ramaswamy, "A variational finite-difference method for analyzing channel waveguides with arbitrary index profiles," *IEEE J. Quantum Electron.*, vol.22, pp.968-976, 1986.
14. K. S. Chiang, "Review of numerical and approximate methods for the modal analysis of general optical dielectric waveguides," *Opt. Quantum Electron.*, vol.26, pp. S113-S134, 1994.
15. T Wolf, C.-L. Shich, R. Engelmann, K. Alavi, and J. Mantz. "Lateral refractive index step in GaAs/AlGaAs multiple quantum well waveguides fabricated by impurity-induced disordering." *Appl. Phys.. Lett.*, vol.55. pp. 1412-1414, 1989.
16. K. B. Kahan and G. Rajeswaran, "Study of the interdiffusion of GaAs-AlGaAs interfaces during rapid thermal annealing of ion-implanted structures" *J. Appl. Phys.*, vol. 66, pp.545-551, 1989.
- 17 E. H. Li, B. L. Weiss, K. S. Chan, and J. Micallef, "Polarization dependent refractive index of an interdiffusion induced AlGaAs/GaAs quantum well", *Appl. Phys. Lett.*, vol. 62, pp. 550-552, 1993.

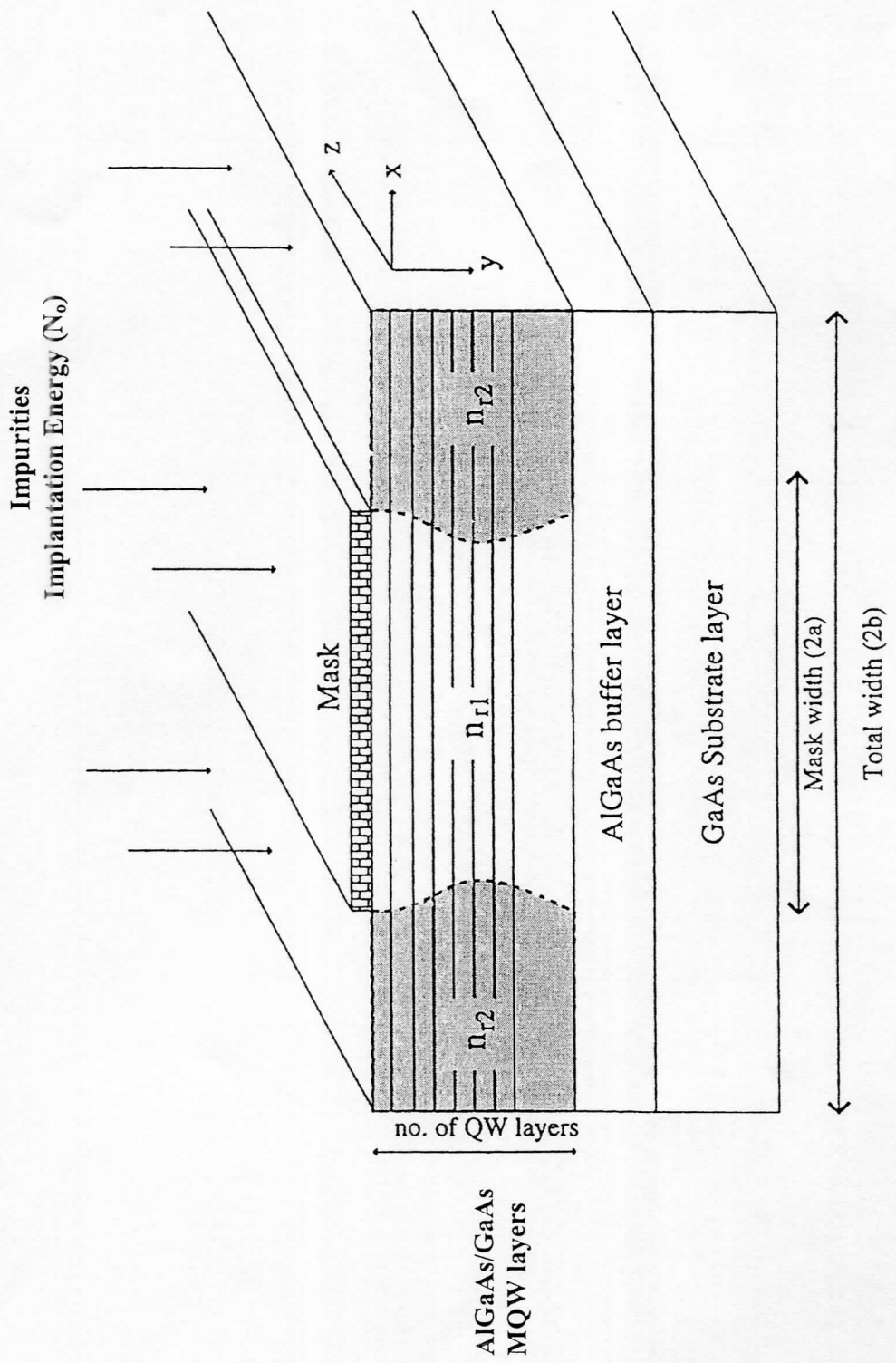


Figure 1 The schematic cross section of IID MQW waveguide

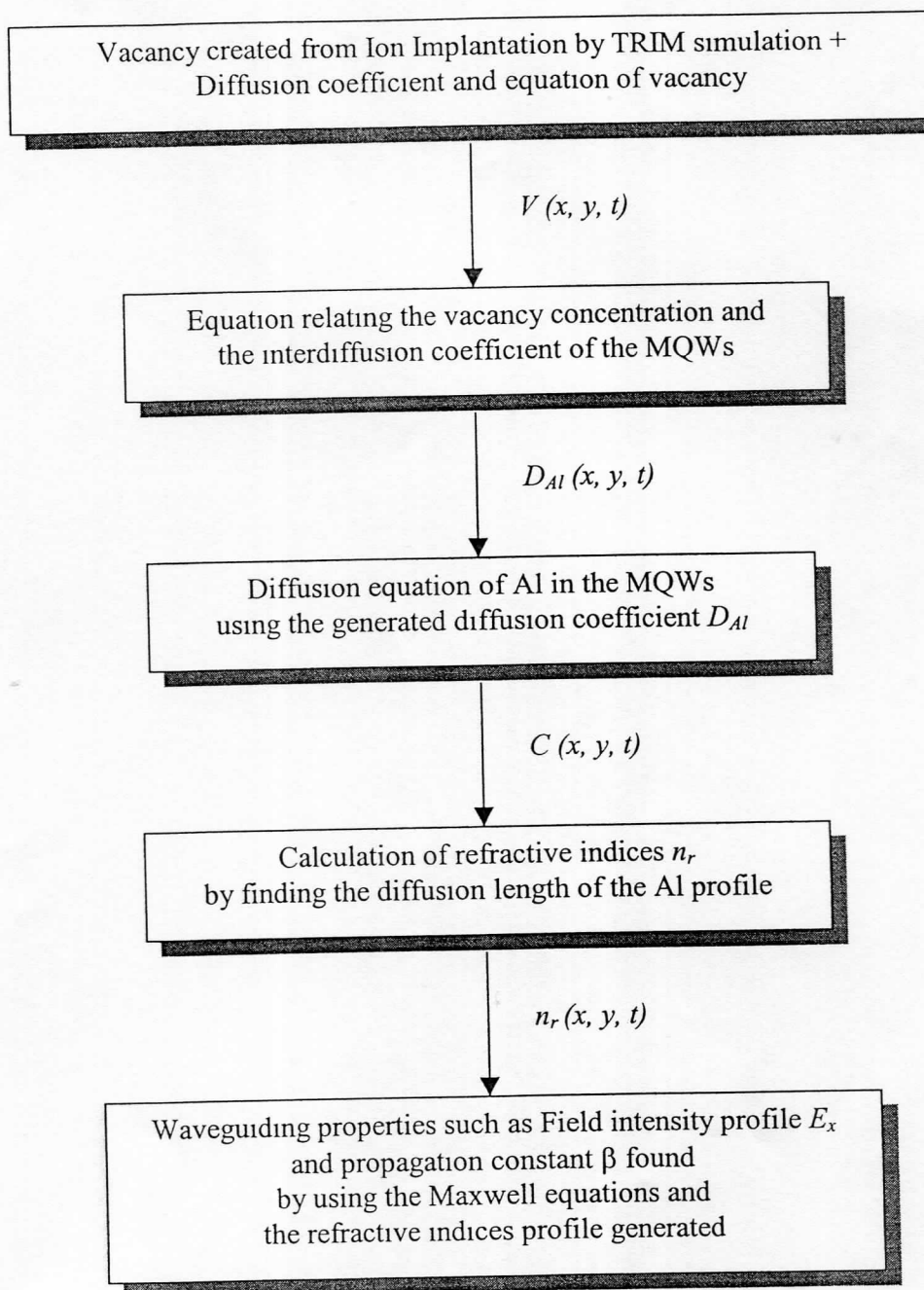


Figure 2 Flow chart to describe the implementation of the model

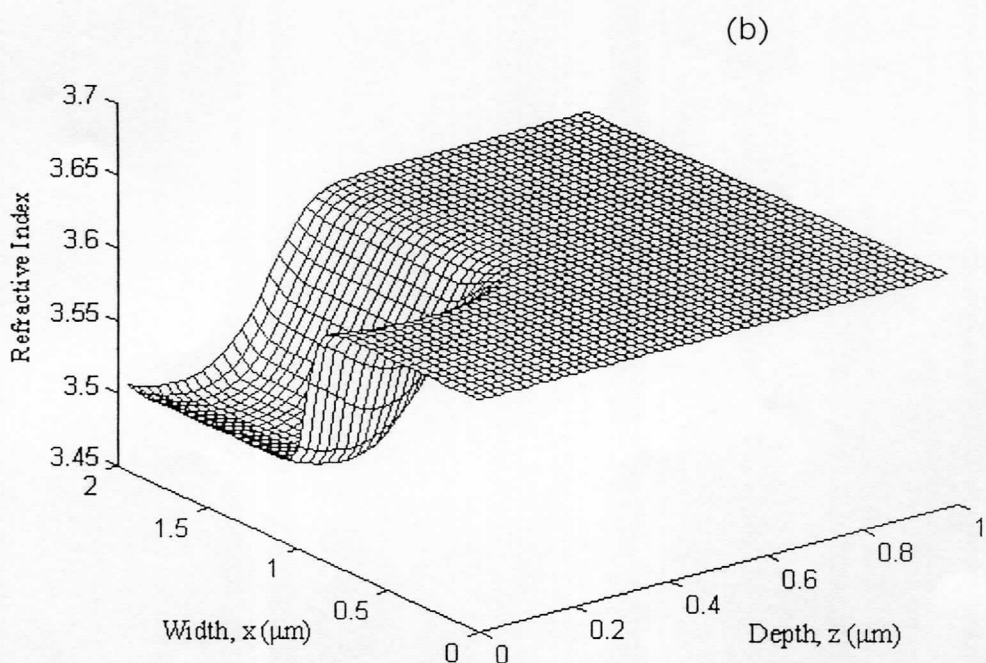
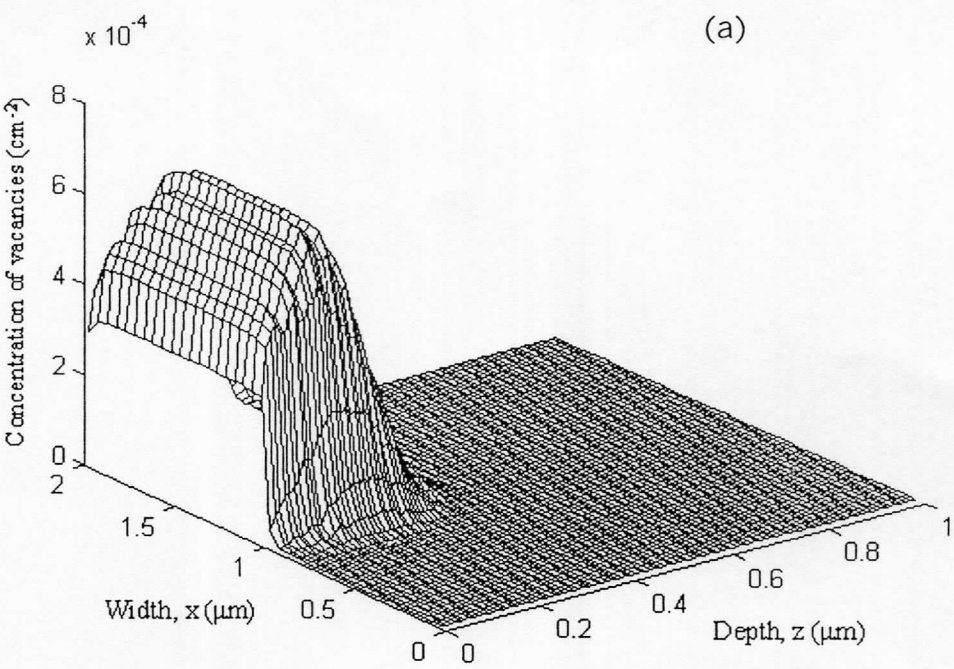


Figure 3 (a) Vacancy profile (b) refractive index profile (both half symmetry) by ion implantation with 220keV, mask width 2 $\mu\text{m}$  and 50 periods of MQWs.

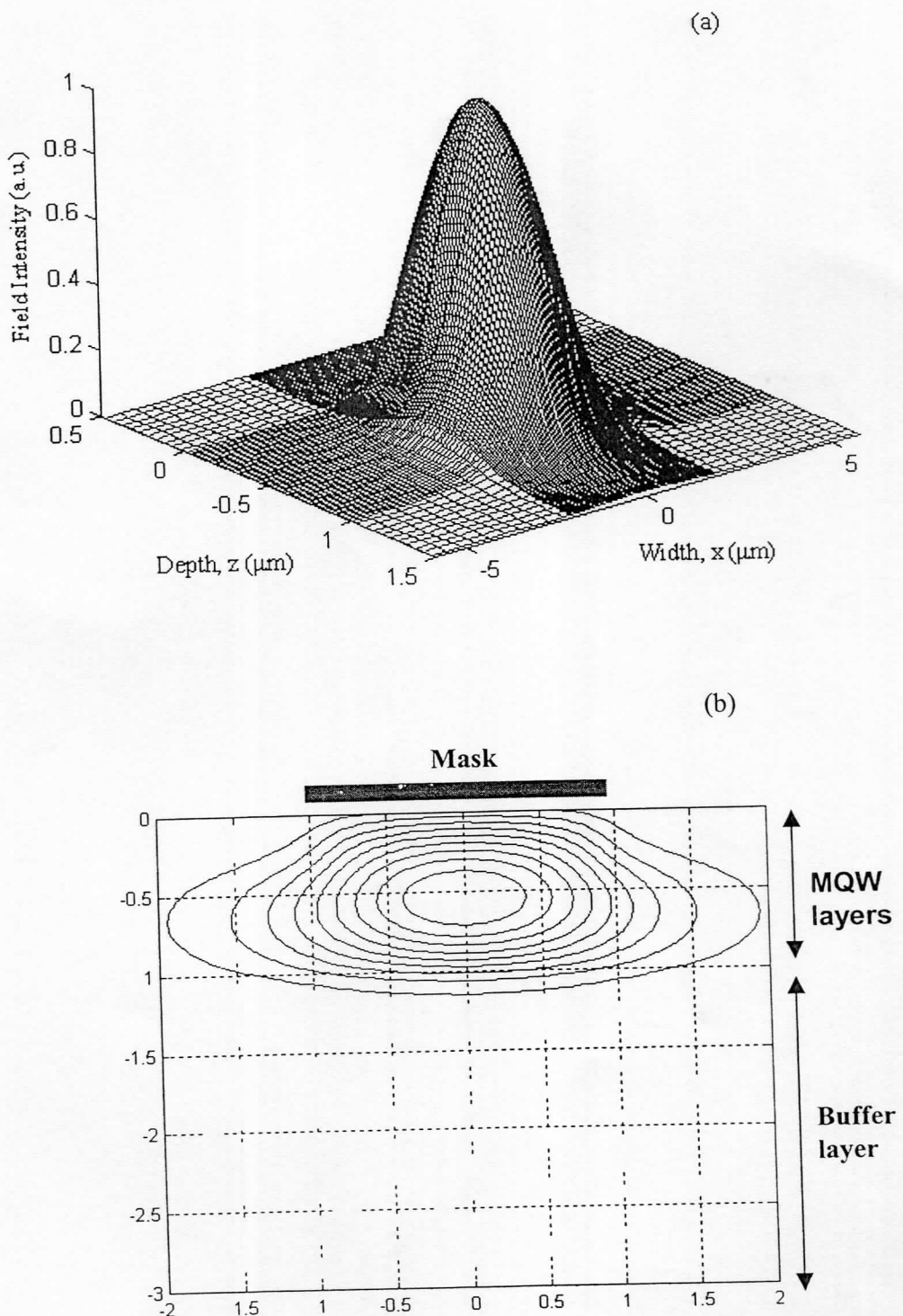


Figure 4 (a), (b) Symmetric  $E_{11}$  field profile as determined by FDM with 50 periods of MQWs layers (i.e. thickness of  $1\mu\text{m}$ )

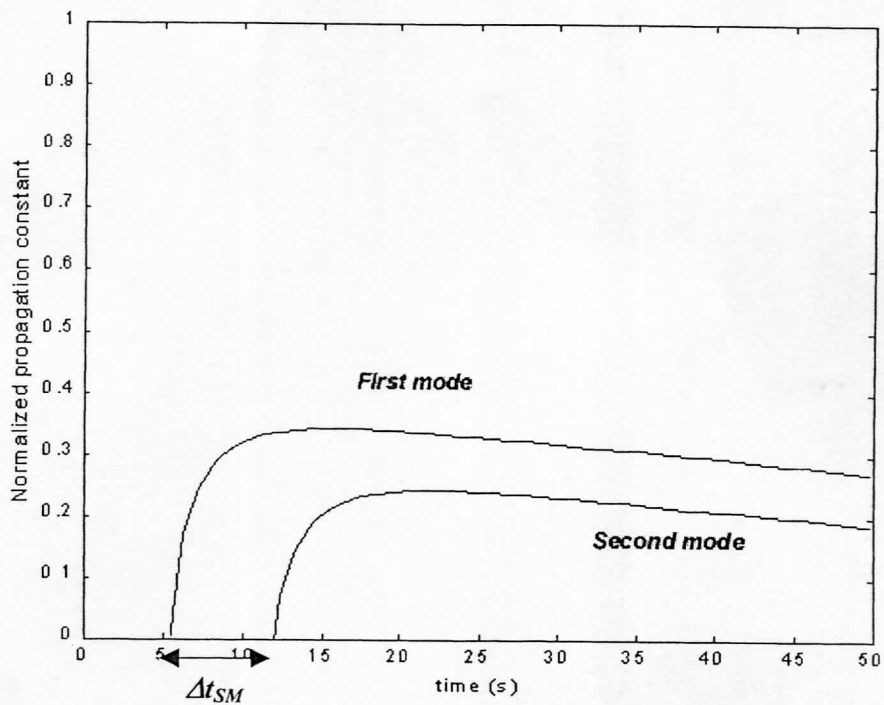


Figure 5 Normalized propagation constant as a function of time obtained from refractive index profile of Figure 3. The starting time for the first guided mode ( $t_1$ ) is 5.1s, and the maintenance time of this single mode ( $\Delta T_{SM}$ ) is 7s.

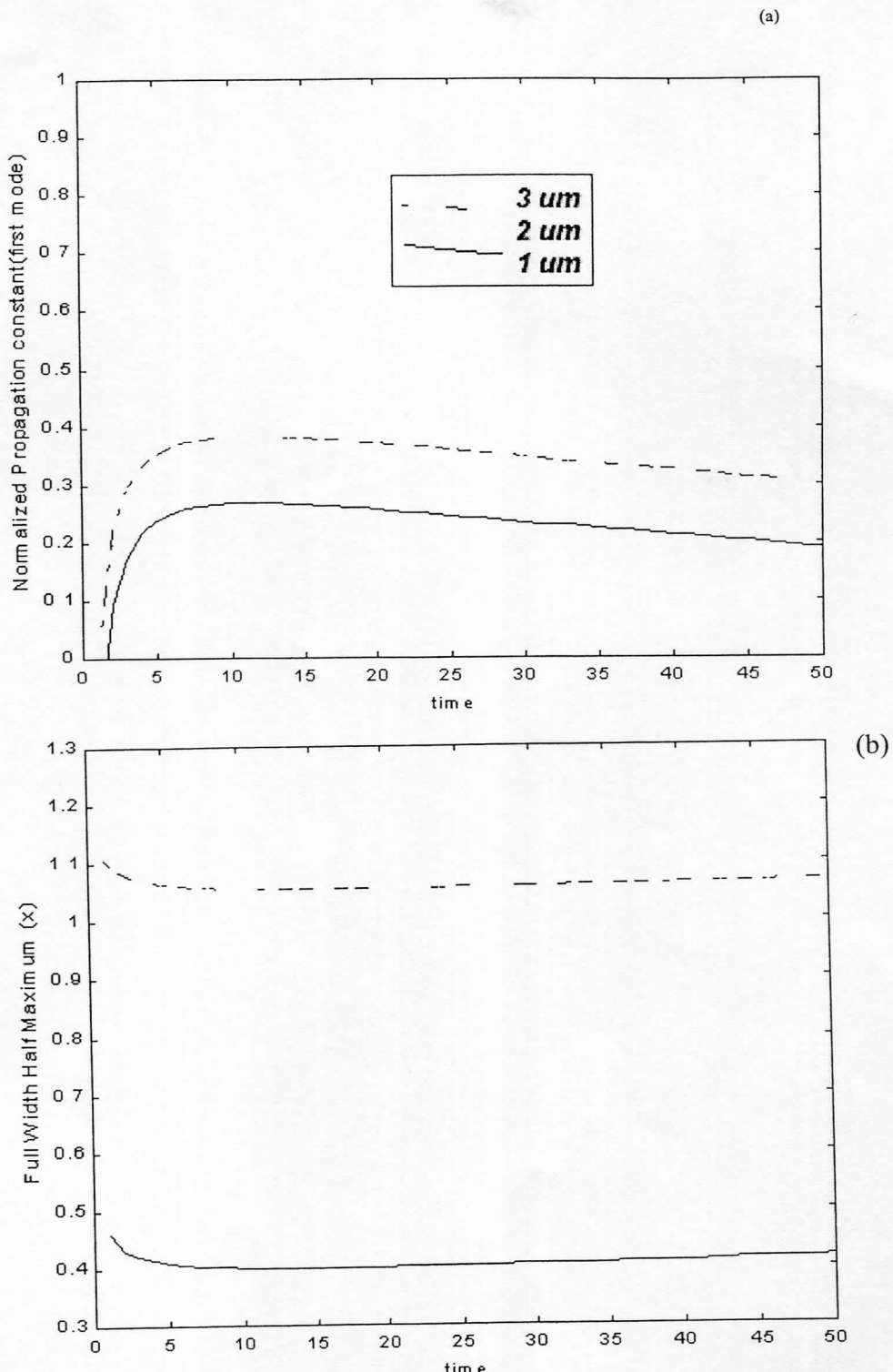


Figure 6

(a), (b) Plot of Normalized propagation constant and FWHM against time with mask width ( $1 \mu\text{m}$ ,  $2\mu\text{m}$  and  $3\mu\text{m}$ ), implant energy =  $220\text{keV}$ ,  $\lambda=0.85 \mu\text{m}$  and 30 quantum wells.

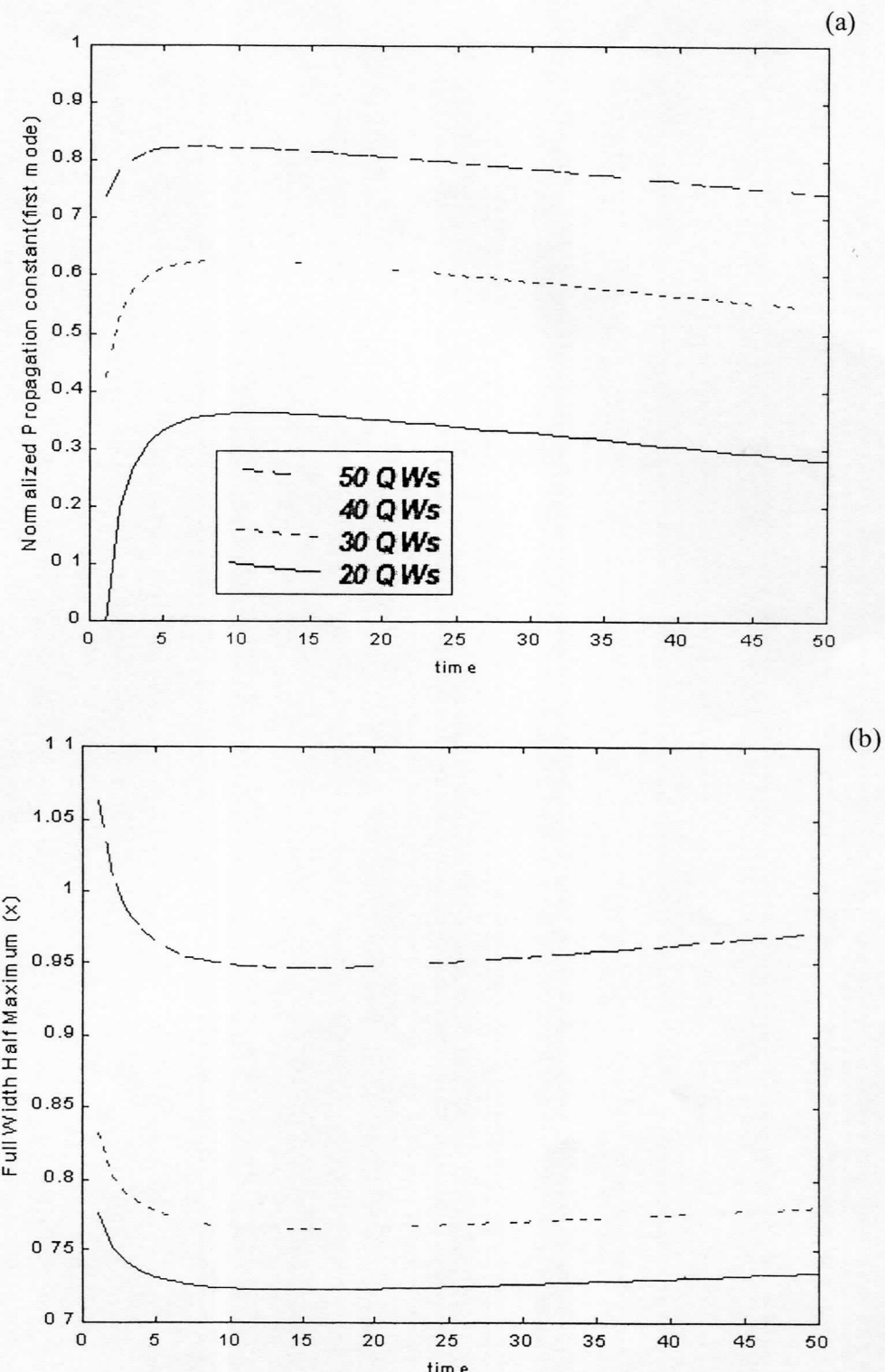


Figure 7  
(a), (b) Plot of Normalized propagation constant and FWHM against time with MQWs periods of (20, 30, 40 and 50) and implant energy of 220keV,  $\lambda=0.85$   $\mu\text{m}$  and mask width=2  $\mu\text{m}$ .

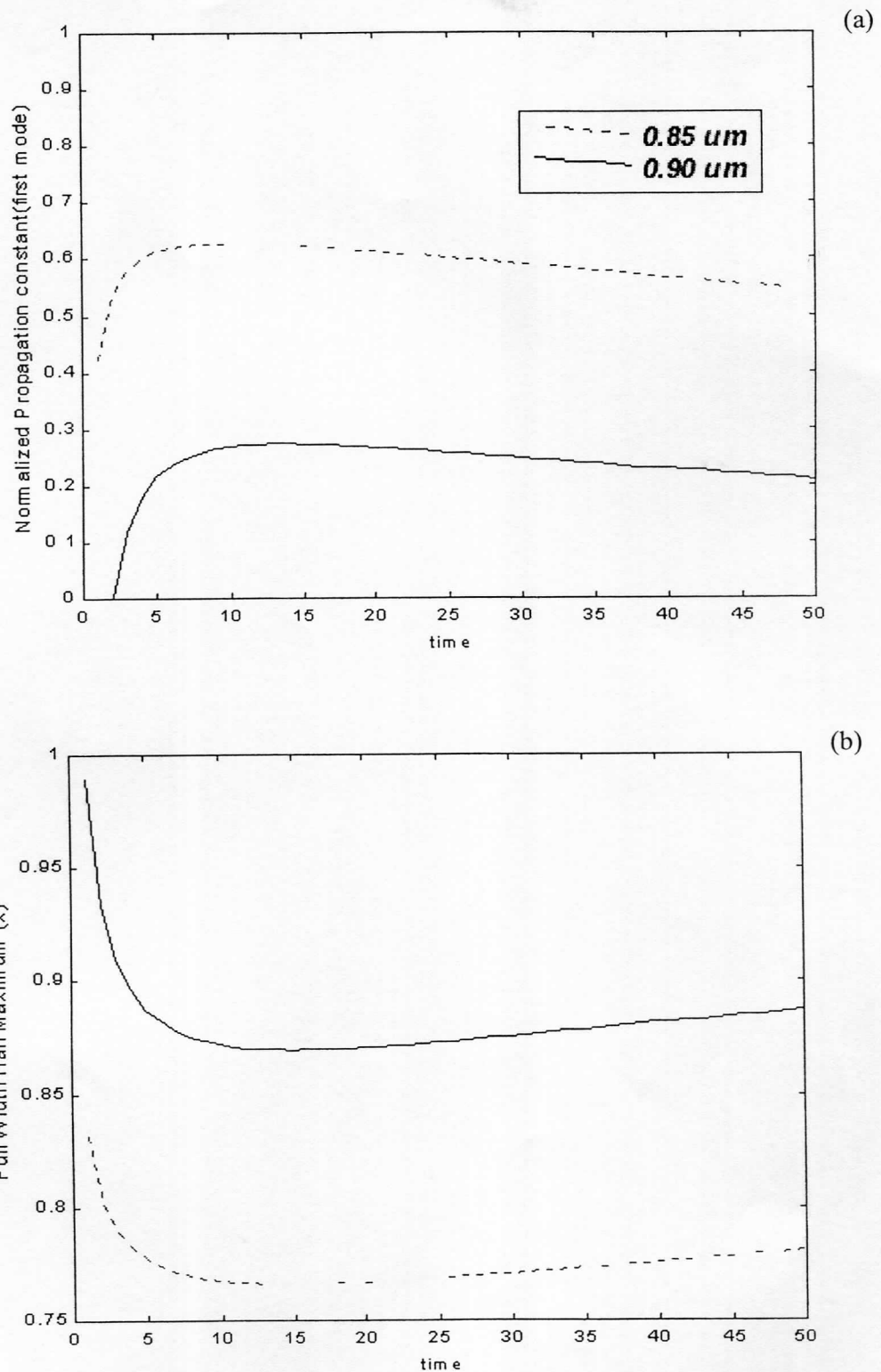


Figure 8

(a), (b) Plot of Normalized propagation constant and FWHM against time at two wavelength ( $0.85\mu\text{m}$  and  $0.9\mu\text{m}$ ), implant energy of  $220\text{keV}$ ,  $\lambda=0.85\mu\text{m}$  and mask width= $2\mu\text{m}$  and 30 quantum wells.

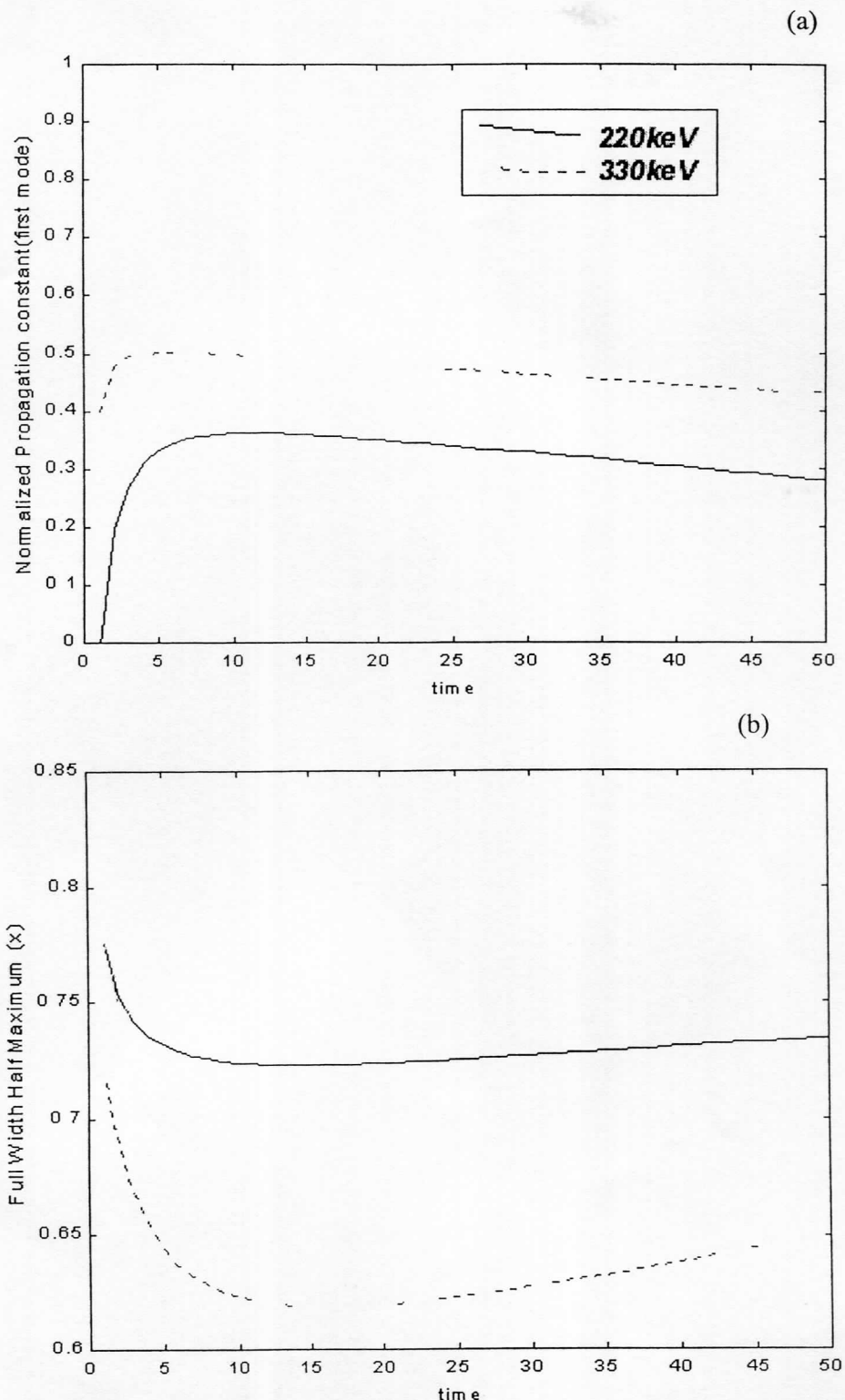


Figure 9

(a), (b) Plot of Normalized propagation constant and FWHM against time with two implantation energy (220keV and 330keV), mask  $(2a)=2\mu\text{m}$ ,  $\lambda=0.85\mu\text{m}$  and 30 quantum wells.